International Journal of Crashworthiness

ISSN: 1358-8265 (Print) 1754-2111 (Online) Journal homepage: https://www.tandfonline.com/loi/tcrs20

Effect of hexagonal on the in-plane crushing behaviour of plain weave composite hexagonal quadruple ring system

E. Mahdi, Munir Faraj, A. M. S. Hamouda, S. M. Sapuan, M. A. Attia & E. O. Eltai

To cite this article: E. Mahdi, Munir Faraj, A. M. S. Hamouda, S. M. Sapuan, M. A. Attia & E. O. Eltai (2020) Effect of hexagonal on the in-plane crushing behaviour of plain weave composite hexagonal quadruple ring system, International Journal of Crashworthiness, 25:2, 192-202, DOI: 10.1080/13588265.2018.1555025

To link to this article: https://doi.org/10.1080/13588265.2018.1555025

Published online: 23 Feb 2019.

INTERNATIONAL JOURNAL OF CRASHWORTHINESS
2020, VOL. 25, NO. 2, 192–202
https://doi.org/10.1080/13588265.2018.1555025

Taylor & Francis
Taylor & Francis Group

Effect of hexagonal on the in-plane crushing behaviour of plain weave composite hexagonal quadruple ring system

E. Mahdi[a], Munir Faraj[b], A. M. S. Hamouda[a], S. M. Sapuan[b], M. A. Attia[c,d] and E. O. Eltai[a]

[a]Department of Mechanical and Industrial Engineering College of Engineering, Qatar University, Doha, Qatar; [b]Department of Mechanical and Manufacturing Engineering, University Putra Malaysia, Serdang, Selangor, Malaysia; [c]Mechanical Design and Production Engineering Department, Faculty of Engineering, Zagazig University, Zagazig, Egypt; [d]Mechanical Engineering Department, College of Engineering, Shaqra University, Dawadmi, Ar Riyadh, Saudi Arabia

ABSTRACT
In this study, an experimental investigation into the crushing behaviour of one dimensional composite hexagonal cellular structure between two plates has been carried out. The materials have been used to accomplish the studies are the plain weave E-glass fabric and the epoxy resin. The tested cellular structures are composed of 4×1 hexagonal cells with angles varied between 35° and 60°. Various crashworthiness parameters of the tested cellular structures such as crushing load capacity, energy absorption capability and force efficiency were computed and discussed. The crush failure modes of the tested rings were identified and analysed. Results showed that the hexagonal ring angle has a significant effect on the crush failure loads and energy absorption capability. Increasing the cell angle showed a decrease in energy absorption capability and load carrying capacity. Additionally, the cell angle has a remarkable effect on the failure sequence of the ring cells.

ARTICLE HISTORY
Received 20 April 2017
Accepted 27 November 2018

KEYWORDS:
Plain weave glass fiber; hexagonal cellular structure; cell-wall angle; crushing behaviour

1. Introduction

In the design and testing of various types of vehicles, crashworthy protection has become a challenging issue. The term 'crashworthiness' refers to the quality of response of a vehicle when it is involved in or undergoes an impact. The less damaged the vehicle and its occupants and contents after a given event, the higher the crashworthiness of the vehicle or the better its crashworthy performance Johnson and Walton [1]. Also, when it comes to energy absorption, the cellular porosity feature is desirable since it can give a long, nearly constant plateau force level under compression. Several studies investigated theoretically, numerically and experimentally the crushing behaviour of thin-walled curved shells constructed from Fiber-Reinforced Polymers [2–10]. This finding can be attributed to their ability to withstand axial loading in a membrane manner rather than through bending [11]. In addition to the vehicle applications, FRP cylinders/tubes are now widely used in chemical plants, oil and gas carriers and high-pressure containers [12,13]. Moreover, the FRP composite gives rise to environmental pollution due to their non-degradability. Gupta and Abbas [14] investigated the quasi-static lateral crushing of composite cylindrical tubes between flat platens; they found that the GFRE tubes have exhibited an effective and stable energy absorption phenomenon in the laboratory testing. The energy absorption capability of FRP composite structures is strongly affected by the mechanical properties of the wall material, wall thickness and geometric parameters of the structure [15–17]. Mamalis et al. [18] investigated the deformation modes and energy absorption of square woven carbon FRP tubes under axial quasi-static and dynamic compressive loads. It was concluded that the peak force increased with the number of layers, wall thickness and fiber volume percentage. Three failure modes were observed; a progressive brittle failure mode, an unstable wall buckling failure mode and a mid-length failure mode. However, the composite structures that failed with a progressive, stable failure mode absorbed more energy than structures that failed with other deformation modes. The behaviour of polyurethane foam filled steel hat sections under axial loading was investigated by Haorongbam et al. [19], results showed that for a minimal increase in weight foam filled steel hat sections can absorb more energy as compared to hollow steel hat sections. Specifically for a 15.63% increase in mass of empty hat sections due to foam filling. Depending on the type of hat sections, the authors concluded that energy absorption increases from 37% to 66%. Elgalai et al. [20] investigated the effect of geometry and material properties on the crashworthiness behaviour of laminated corrugated tubes. Alkateb et al. [5] and Mahdi et al. [21] investigated the crashworthiness behaviour of core and coreless composite elliptical thin-wall cones and tubes with different ellipticity ratio and vertex angles, respectively, under quasi-static axial compression. The specimens were made from woven roving glass fiber with the orientation of [0/90] and epoxy resin, whereas natural cellular

CONTACT E. Mahdi elsadigms@qu.edu.qa
This article has been republished with minor changes. These changes do not impact the academic content of the article.

fiber was used as filler for the core tubes. It is worth remarking that geometrical parameters significantly influenced the energy absorption capabilities and failure modes. Abosbaia et al. [13,22] analysed the segmentation influence on the crushing behaviour and collapse modes of segmented and non-segmented tubes subjected to axial and lateral loads. The tubes were made from glass mat, carbon fabric fiber and cotton fabric fiber with epoxy resin. Mahdi and Hamoouda [23] studied the energy absorption capabilities of woven roving glass/epoxy hexagonal ring systems. They concluded that the ring geometry has a significant effect on the crashworthiness performance of composite quadruple hexagonal ring system. Triggering is a geometric gradient feature in the component as it acts as a stress concentration to ensure the collapse initiation. Jimenez et al. [24] demonstrated the influence of a trigger mechanism on the energy absorbed and progressive collapse of FRP composite structures. Eshkoor et al. [25] investigated the crushing behaviour of woven natural silk/epoxy triggered composite rectangular tubes subjected to an axial quasi-static crushing test. It was concluded that the tube thickness and length have a remarkable effect on the crashworthiness performance. Mahdi et al. [26] investigated the effect of fiber content on the energy absorption capability of axially crushed E-glass woven fabric/epoxy resin composite tubular. Moreover, Sebaey et al. [27] investigated the crashworthiness characteristics of hybrid octagonal and hexagonal carbon fiber reinforced epoxy composite system. Mahdi and Sebaey [4] examined the effect of aramid fiber composite on the crashworthiness of composite octagonal and hexagonal systems. Alkbir et al. [28,29] studied the effect of geometry on the crashworthiness parameters of natural kenaf FRP composite hexagonal tubes under axial and lateral crushing loads. They found that the hexagonal angle of the composite tube has a remarkable effect on the specific energy (E_s) absorption capability. Chiu et al. [30] studied the behaviour of a carbon-epoxy composite energy absorber under static and dynamic loading. The energy absorption was found to be independent of strain rate within the studied range $100\,s^{-1}$. Esnaola et al. [31] analysed the effect of the fiber volume fraction on the energy absorption capability of glass/polyester. They found that by increasing the fiber volume fraction from 40% to 47%, the specific energy (E_s) absorption increased to 56 kJ/kg. Sun et al. [32] investigated the in-plane crushing and energy absorption performance of multi-layer regularly arranged circular honeycombs. They stated that the energy absorbed per unit volume is significantly controlled by the dynamic plateau stress and dynamic densification strain. They also found that the energy absorption capacity is proportionally reversed with the dynamic densification strain. Hussein et al. [33] evaluated the response of axially compressed CFRP composite square tubes. They found that the deformation mode of 100 mm long CFRP tubes was a catastrophic failure, while the deformation mode of 50 mm long CFRP tubes was a progressive collapse. Wang et al. [34] investigated the collapse characteristics and energy absorption capability of carbon fiber/epoxy composite tubes under axial quasi-static and impact crushing conditions. Brittle fracturing has been identified as the dominated failure mechanism. From the reviewed literature, one can conclude that few studies have been conducted to address the energy absorption capability of hexagonal array systems. The gap in this field is the main reason behind this study, in which the main objective is to investigate the effect of hexagonal angle on the crashworthiness parameters of 4×1 cellular ring systems.

2. Experimental program

2.1. Materials and specimens preparation

The specimens were employed in this study made of plain weave fiber-reinforced epoxy. The ratio of epoxy resin to hardener was 5:1. The main advantage of using plain weave fabric laminates is that they provide properties that are more balanced in the [0°/90°] directions than unidirectional laminates. These balanced properties are attributed to the fact that the circumferentially (90°) oriented fibers reduce the interlaminar stresses between layers while supporting the longitudinally oriented fibers (0°) to carry the applied load. These findings were also supported by Mahdi et al. [12] and Mahdi and Hamouda [23]. The wet wrapping process was used to fabricate the specimens. More details about the fabrication method can be found in Mahdi et al. [12,26]. Tables 1 and 2 give the geometrical and physical properties of fabricated specimens and materials Properties of glass fiber plain weave/epoxy composite. The average fiber volume fraction was found to be 0.55%. Six configurations with different cell angles varied between 35° and 60° were fabricated and tested to evaluate the crashworthiness performance of composite quadruple hexagonal ring systems as shown in Figure 1.

2.2. Quasi-static test

The test setup is sketched in Figure 2. Quasi-static tests were performed to assess the crashworthiness performance and monitor the crushing mechanisms of the quadruple system. INSTRON 8500 digital-testing machine with a full-scale load range of 250 kN was used for quasi-static compression tests. Steel plates were set parallel to each other before the initiation of the test. For data reproducibility, five samples of each configuration were tested, and the mean

Table 1. Geometrical characteristics of the test matrix.

Configuration*	Angle β (degree)	a (mm)	b (mm)	Thickness t (mm)	Height (mm)	Weight (g)
Hx-35	35	25	60	1.49	178.8	105.8
Hx-40	40	26	58	1.50	180.0	106.3
Hx-45	45	30	50	1.52	182.4	107.5
Hx-50	50	32	46	1.51	181.2	106.5
Hx-55	55	35	40	1.50	180.0	105.3
Hx-60	60	40	30	1.47	176.4	107.3

value was considered as the final result. The behaviour of each configuration under compression loading was recorded using a digital camera. The acquisition system of the universal testing machine recorded the load-displacement data at a constant crosshead speed of 5 mm/min.

Table 2. Materials Properties of glass fiber plain weave/epoxy composite.

	Plain weave glass fiber/epoxy
Fiber volume fraction	0.55
Density (g/m^3)	1.85
Longitudinal modulus (GPa)	26
Transverse modulus (GPa)	22
Shear Modulus (GPa)	7.2
Poisson's ratio	0.13
Longitudinal tensile strength (MPa)	166.7
Longitudinal compressive strength (MPa)	145.8
Transverse tensile strength (MPa)	158.3
Transverse compressive strength (MPa)	116.7
In-plane shear strength (MPa)	18.75

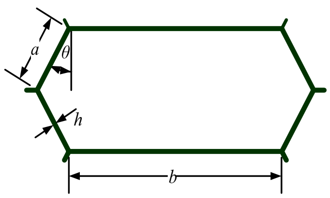

Figure 1. Geometry of the hexagonal cell under investigation.

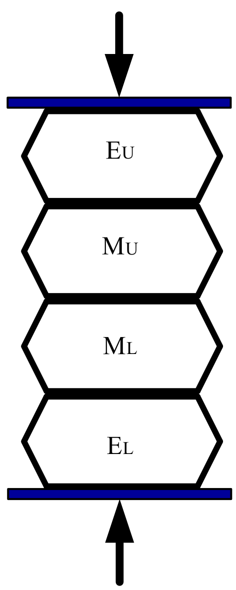

Figure 2. The in-plane crushing of quadruple hexagonal system.

2.3. Crashworthiness parameters

Human and environmental factors are the primary cause of Motor vehicle accidents. By employing proper safety design and manufacturing techniques, automobile manufacturers can prevent many of the deaths and serious injuries that result from accidents. One of these preventive strategies is to utilise a collapsible energy absorber device; this can be achieved by converting the impact energy into plastic deformation energy in the case of metal-based energy absorber devices and into fracture deformation in the case of composite-based energy absorber devices. Therefore, fatal injuries can be avoided keeping the peak force exerted on the protected occupants below their tolerance level, long deformation path to sufficiently reduce the deceleration of the protected occupants can be provided by the collapsible energy absorber devices. The specific energy (E_s) absorption is a critical factor to evaluate the crashworthiness of an energy absorber device, and it can be defined as the total work done per unit mass of material. The entire work is done (W_T) or energy absorbed is the area under the load–displacement curve and can be computed as:

$$W_T = \int_0^{s_b} Pds \tag{1}$$

In this study, only the work done (W) during the post-crush stage will be considered. Therefore, one can rewrite Equation (1) as follows:

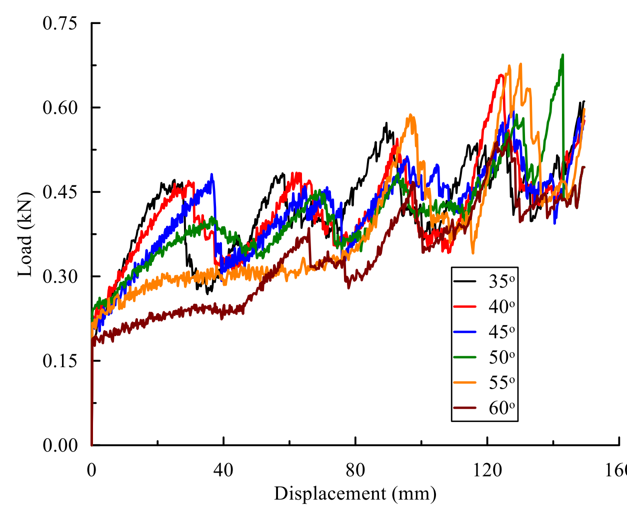

Figure 4. The load-displacement curves for composite hexagonal quadruple ring system with different hexagonal angles.

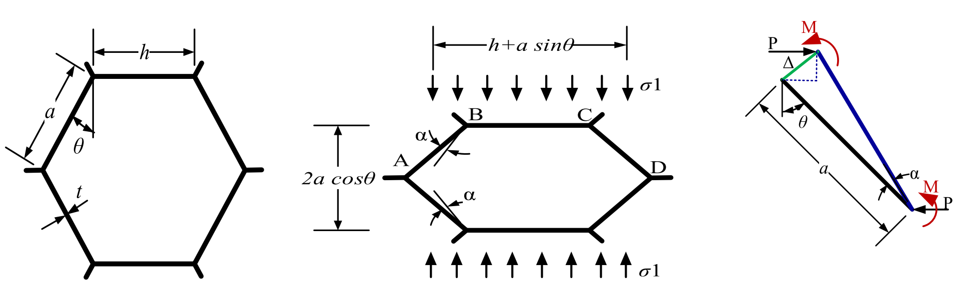

(a) (b) (c)

Figure 3. Cell deformation by cell wall bending caused by crush loads in the x-direction.

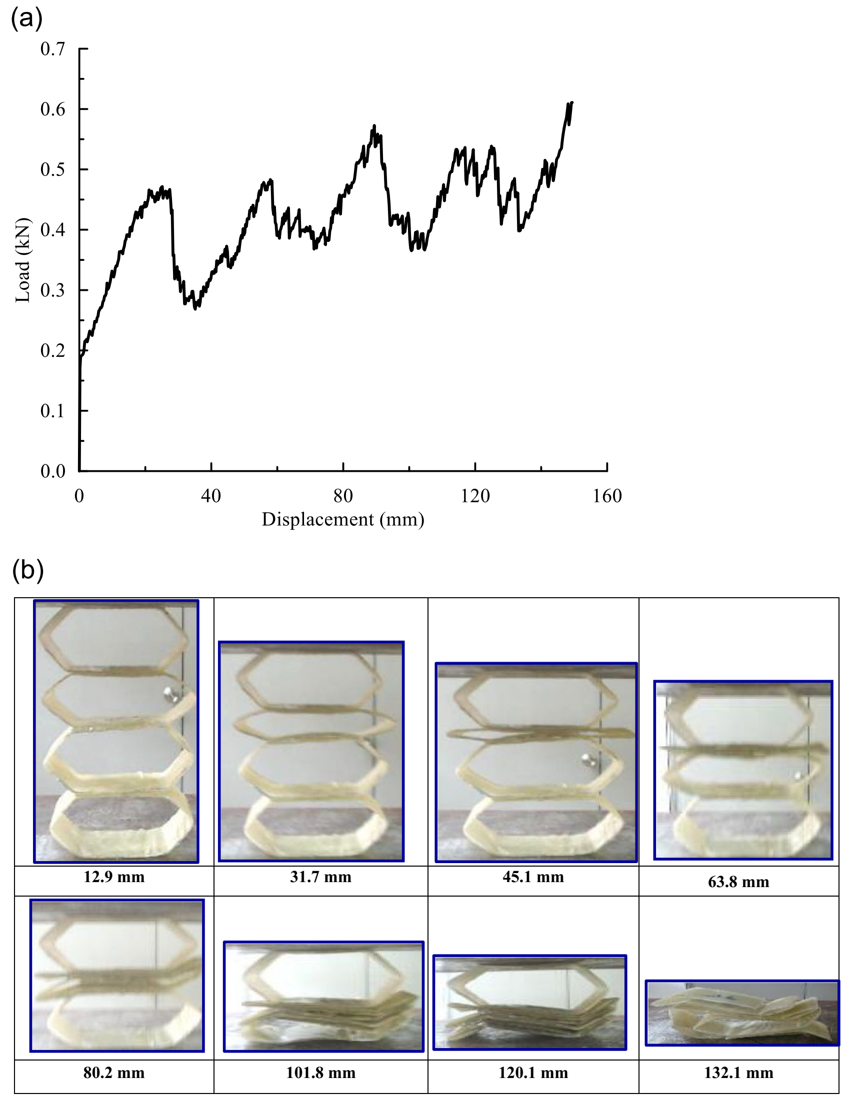

Figure 5. (a) The load-displacement curve for composite hexagonal quadruple ring system with angle 35°. (b) Representative-photographs have been taken during different stages of deformation history of composite hexagonal quadruple ring system with angle 35°, crushing sequence (M_U-M_L-E_L-E_U).

$$W = \int_{s_i}^{s_b} P ds = P_m(s_b - s_{bi}) \quad (2)$$

where S_b and S_i are the crush distances and P_m is the mean/average crush load. The specific energy (E_s) absorption capability, E_s, of a composite material defined as the energy absorbed per unit mass of material is given by:

$$E_s = \frac{W}{M} = \frac{P_m(s_b - s_i)}{M} = \frac{P_m(s_b - s_i)}{M} \quad (3)$$

where, M is the mass of the structure being investigated.

3. Design requirements

Improving the safety and optimising the weight of composite energy absorber devices are the driving forces for the design of high-performance composite energy absorber. Two design parameters have been used to explore and study the crashworthiness performance of composite quadruple systems. The first parameter is the geometry configuration in which six angles were used. The quadruple angles varied between 35° and 60° with an increment of 5. The second parameter is the effect of a hexagonal system arrangement, in which two different methods have been used. The energy absorber device must be designed to alleviate the impact of the accident into a predetermined stable energy absorption mechanism. The excellent energy absorption mechanism is a progressive failure mechanism. For thin walled structures such as cellular structure composed of hexagonal cells, the possibility of global (Euler) buckling exists, because it leads to catastrophic failure mechanism. Therefore, any energy absorbing system design must assure the elimination of global buckling as energy absorbing mechanism by maximising the bending stiffness, which is the product of the axial modulus of elasticity and the moment of inertia of the cell wall, because it increases the critical load directly. Accordingly, the cellular dimensions are selected due to the vehicle space limits. In this design requirement, the cellular must absorb the energy while the crushing force and stroke efficiencies are stable and high, respectively. In the following, the relationship between plastic stress and cell geometry will be derived. The external work was done by the force

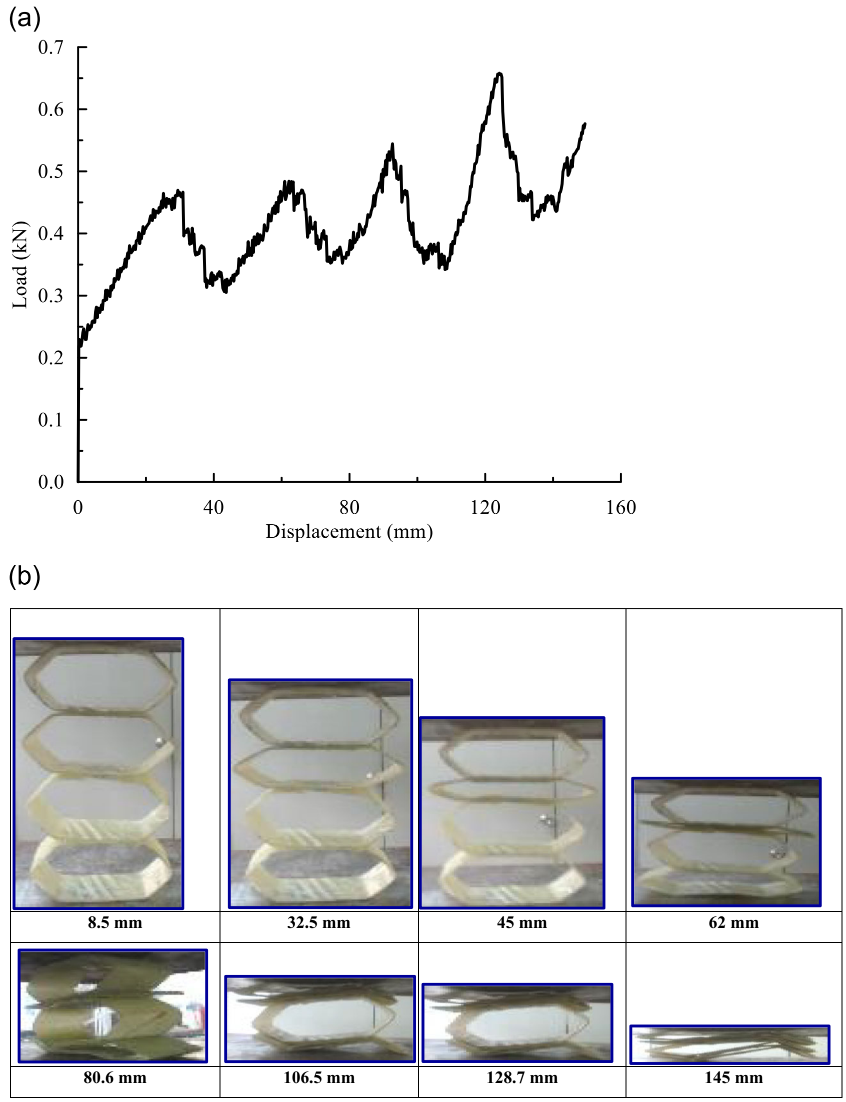

Figure 6. (a) The load–displacement curve for composite hexagonal quadruple ring system with angle 40°. (b) Representative-photographs have been taken during different stages of deformation history of composite hexagonal quadruple ring system with angle 40°, crushing sequence (M_U-E_U-E_L-M_L).

induced by σ_1 during a plastic rotation α of the four hinges A, B, C and D (Figure 3(b,c)) should be equal to the energy dissipated by these hinges, i.e.

$$[2\sigma_1 b(h + a\sin\theta)a\sin\theta]\alpha = 4M_p\alpha \tag{4}$$

where b is the wall depth.

Term $[\sigma_1 b(h + a\sin\theta)$ is the force at B due to σ_1, in the direction of σ_1 and the plastic bending moment M_p of the cell wall is given by

$$M_p = \frac{\sigma_{ul} b t^2}{4} \tag{5}$$

with σ_{ul} being the ultimate stress of the plain weave glass/epoxy composite and t refers to the wall thickness. From Equations (4) and (5), one can obtain

$$\sigma_p = \sigma_{ul}\left(\frac{t}{a}\right)^2\left[2\left(\frac{h}{a} + \sin\theta\right)\sin\theta\right]^{-1} \tag{6}$$

Also, the relative density ρ and effective modulus of elasticity in the x direction E_x of the structure can be obtained as, Gibson and Ashby (1999)

$$\rho = \rho_s\frac{t}{a}\left(2 + \frac{h}{a}\right)\left[2\cos\theta\left(\frac{h}{a} + \sin\theta\right)\right]^{-1} \tag{7}$$

$$E_x = E_s\left(\frac{t}{a}\right)^2\left[\left(\frac{h}{a} + \sin\theta\right)\sin\theta\tan\theta\right]^{-1} \tag{8}$$

where, ρ_s and E_s are respectively the density and Young's modulus of cell wall material. According to the above equations, it can be deduced that the cellular geometry significantly affect the failure deformation as the structure properties depend on the cell wall properties (σ_{ul} and E_s), cell shape (θ and h/a) and density (t/a). From these equations, one can deduce that the failure deformation is significantly influenced by ring geometry. Generally, the specific energy (E_s) absorption of the ring system increases nonlinearly with displacement and its rate is slower during the initial collapse stage.

4. Results and discussion

The crashworthiness characteristics, deformation patterns and the corresponding load-deformation history of all the plain weave composite quadruple system were studied under quasi-static in-plane lateral compressive loading conditions.

4.1. Load–displacement relationship

Load–displacement curves of the plain weave glass composite hexagonal quadruple system (4×1 cellular structures) with different hexagonal angles (ranged from 35° to 60°) are shown in Figure 4. Figures 5(a)–10(a) show the load–displacement response for the tested specimens. It is clear that each load–displacement curve generally represents three energy absorbing mechanism phases. In the first phase, the ring responds in a linear elastic manner, and this stage terminates when an initial crushing load (P_i) is reached. The second phase represents the post-crush stage, in which, the load carrying capacity fluctuates with troughs over a large range of deformation. Finally, the load carrying capacity increases rapidly, as a result of compaction of hexagonal cells' over each other, which creates material densification. According to the obtained results, the hexagonal angle has significantly affected the load–displacement response of the composite hexagonal cellular structures. Visual observations of the specimens are shown in Figures 5(b)–10(b). As can be seen in the photos, each peak in the load–displacement diagram corresponds to the complete collapse of one cell and the initiation of the damage in the other cells. Similar load–displacement behaviour was obtained for the hexagonal tube and hybrid hexagonal–octagonal cellular systems tested by Mahdi and Hamouda [23] and Sebaey et al. [27].

4.2. Energy absorption capability

Effect of the hexagonal angle on the failure crush loads of plain weave E-glass/epoxy composite hexagonal quadruple system was examined. The specific energy (E_s) absorbed was computed using Equations (1)–(3). Variation of post crushing of the ring systems with their hexagonal angles has been plotted in Figure 11. Accordingly, the calculated specific energy (E_s) absorbed by quadruple hexagonal ring systems decreases with increase in hexagonal angle. Among the

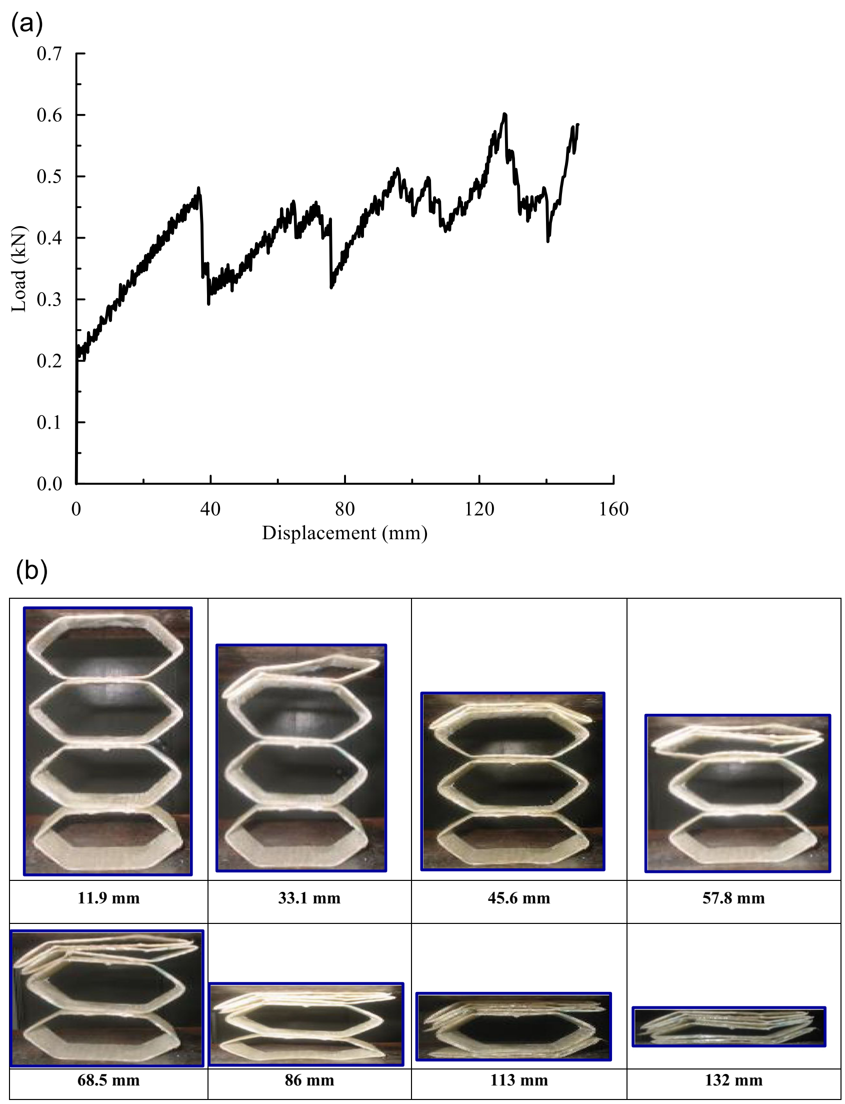

Figure 7. (a) The load–displacement curve for composite hexagonal quadruple ring system with angle 45°. (b) Representative-photographs have been taken during different stages of deformation history of composite hexagonal quadruple ring system with angle 45°, crushing sequence (E_U-M_U-E_L-M_L).

tested specimens hexagonal ring systems with the angle of 35° displayed the highest energy absorbed values of 585 J/kg, while systems angle of 60° recorded the lowest value of 465 J/kg.

4.3. Energy absorbing mechanism

Three energy absorbing mechanism phases were observed. In the first phase, the linear elastic mechanism dominating the energy absorbing capability behaviour of 4×1 quadruple structure. During this phase, both the energy absorption capability and the load carrying capacity increase linearly. This phase ended when the elastic energy and the critical stress were reached, and this attained energy level, and load carrying capacity fluctuates with troughs over a large range of deformation (phase 2). Finally, the load carrying capacity increases rapidly while the energy absorption capability decreases with deformation, because of compaction of hexagonal wall cells over each other [35–37]. The crushing history of the array ring systems is shown in Figures 5(b)–10(b). For the loading direction considered in this study (see Figure 3), there is no elastic buckling in the specified direction. The sides that are fully contacted with the crushing plates are considered as horizontal beams, which resulted in the absence of column effect. For plain weave glass fabric, fracturing was found to be the mechanism governing the post-crash phase. When the inclined side rotates by a small angular increment α, the point in contact with upper beam moves inward with respect to the other point at the end of the inclined side by $(a \sin \theta)\alpha$ as can be seen in Figure 2. This deformation process continued until the end of the post-crush stage. Fracture lines are only observed at the end of the post crush stage and just before the starting of material densification stage. In addition, it was clear from Figures 5(a)–10(a) that quadruple systems exhibited to have a very high carrying capacity. When crushed between two flat plates, the load–displacement response does not show a sharp sudden-drop in load for a large range of deflections, which is advantageous for an

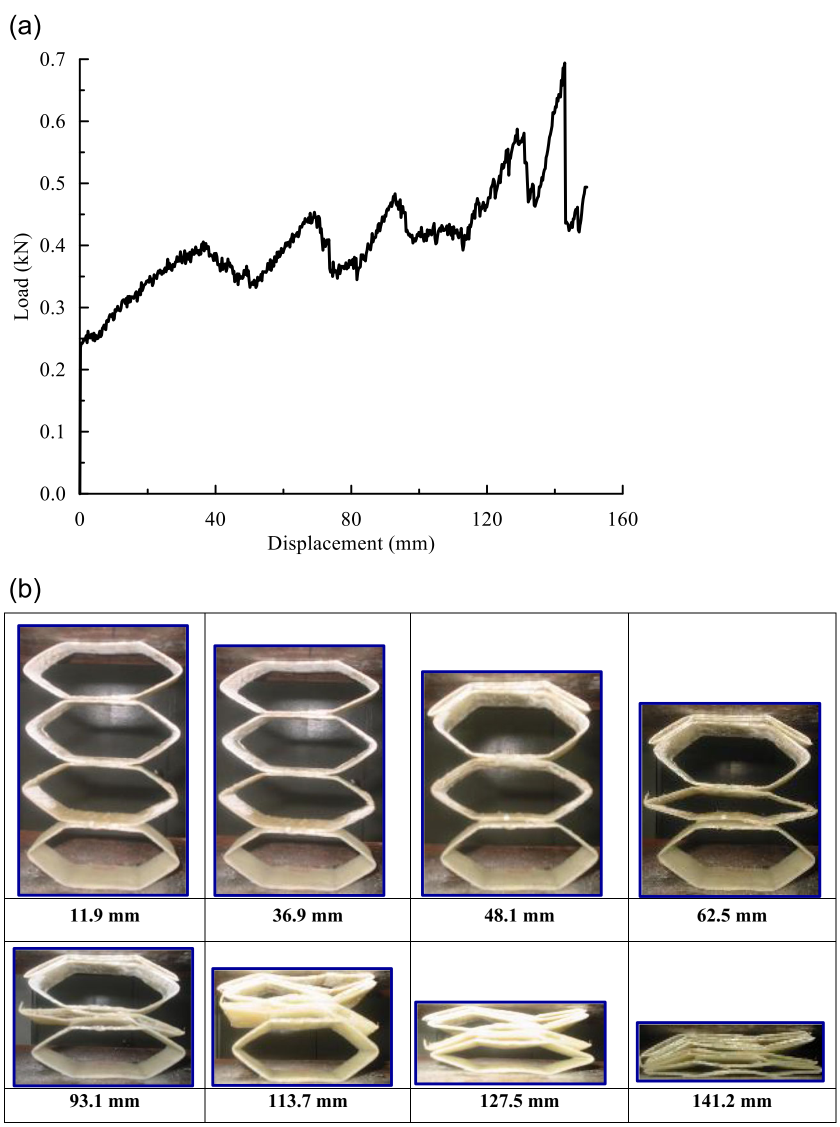

Figure 8. (a) The load–displacement curve for composite hexagonal quadruple ring system with angle 50°. (b) Representative-photographs have been taken during different stages of deformation history of composite hexagonal quadruple ring system with angle 50°, crushing sequence (E_U-M_L-M_U-E_L).

energy-absorber and tends to decrease the deceleration of vehicles occupants. It was observed that the cell geometry has a noticeable effect on the crushing sequence of the ring cells. It is interesting to observe that the third row in system arrays (**M_L**) was not appear as the first crushed row for all hexagonal angles. For low hexagonal angles ($\theta = 35^{\circ}$ and 40°), the second row in the array (**M_U**) was crushed firstly and, the crushing sequence is (**M_U-M_L-E_L-E_U**) and (**M_U-E_L-E_U-M_L**) for $\theta = 35^{\circ}$ and 40°, respectively. This may be attributed to the wall length (h) becomes larger for small angles and, consequently, the contact area between the upper surface of the first row and the platen is increased. This in turn reduced the contact stresses induced on the surface, hence the crushing collapse started away from the upper and lower rows. On the other hand, for large hexagonal angle ($\theta \geq 45^{\circ}$), the contact area became smaller and consequently the, crushing failure started from the upper or the lower cells due to the relatively high contact stress. Also, by increasing the hexagonal angle, a remarkable decrease in the effective modulus of elasticity and an increase in the bending moment were noticed [38]. This in turn leads to high bending stresses and bending deflection.

4.4. Microscopic investigation

Throughout the crushing process, it was considered important to conduct a microscopic investigation to obtaining failure mechanism at the micro level. It was observed that the energy absorbed by the ring is dissipated to crack the matrix at the top end of the specimens. As the crush failure load is further increased, the density and extent of the matrix cracks progress such that interfacial debonding occurs leaving the fibers unsupported, more compliant, and less likely to fail by micro-buckling. Generally, the energy absorbed during this failure stage can be written as follow:

$$W_{micro} = W_{mc} + W_{fd} + W_{bf} \quad (10)$$

where, W_{mc} is the energy required to crack the matrix and increase the density of matrix cracks. It is well understood that in polymer matrix systems, cracks are often initiated at

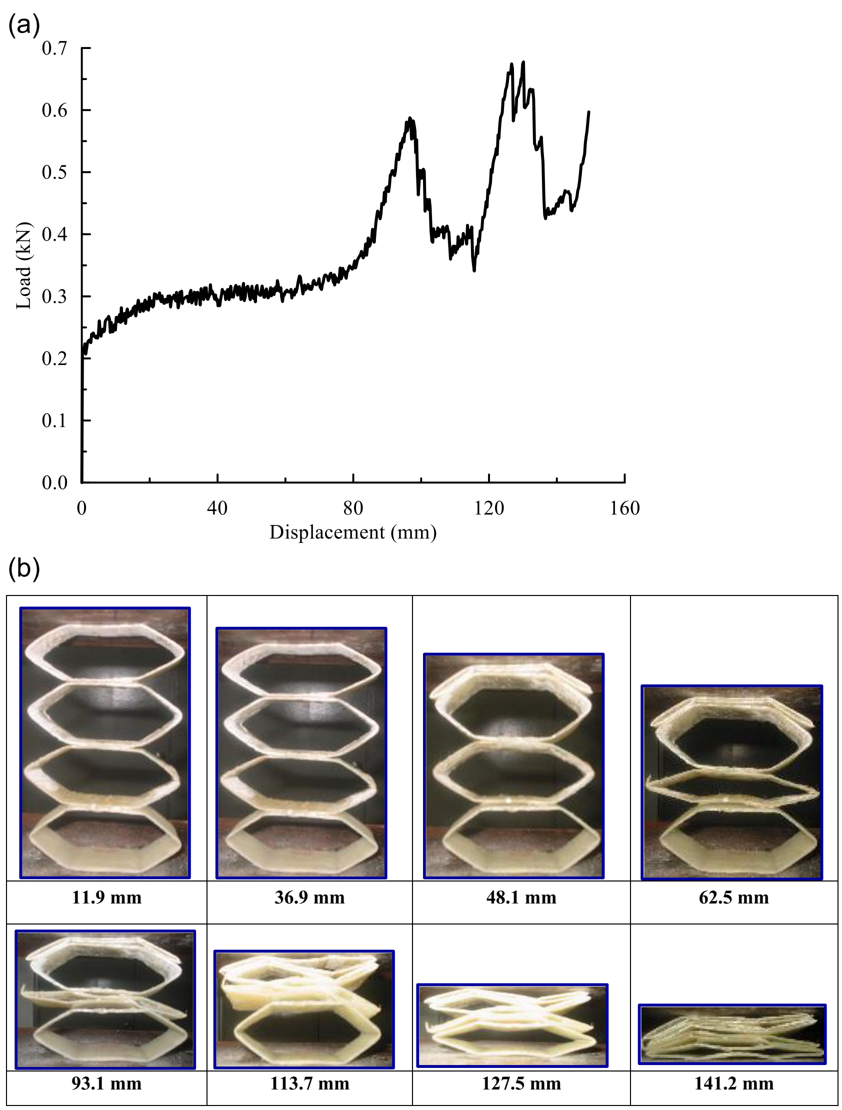

Figure 9. (a) The load–displacement curve for composite hexagonal quadruple ring system with angle 55°. (b) Representative-photographs have been taken during different stages of deformation history of composite hexagonal quadruple ring system with angle 55°, crushing sequence (E_L-M_L-M_U-E_U).

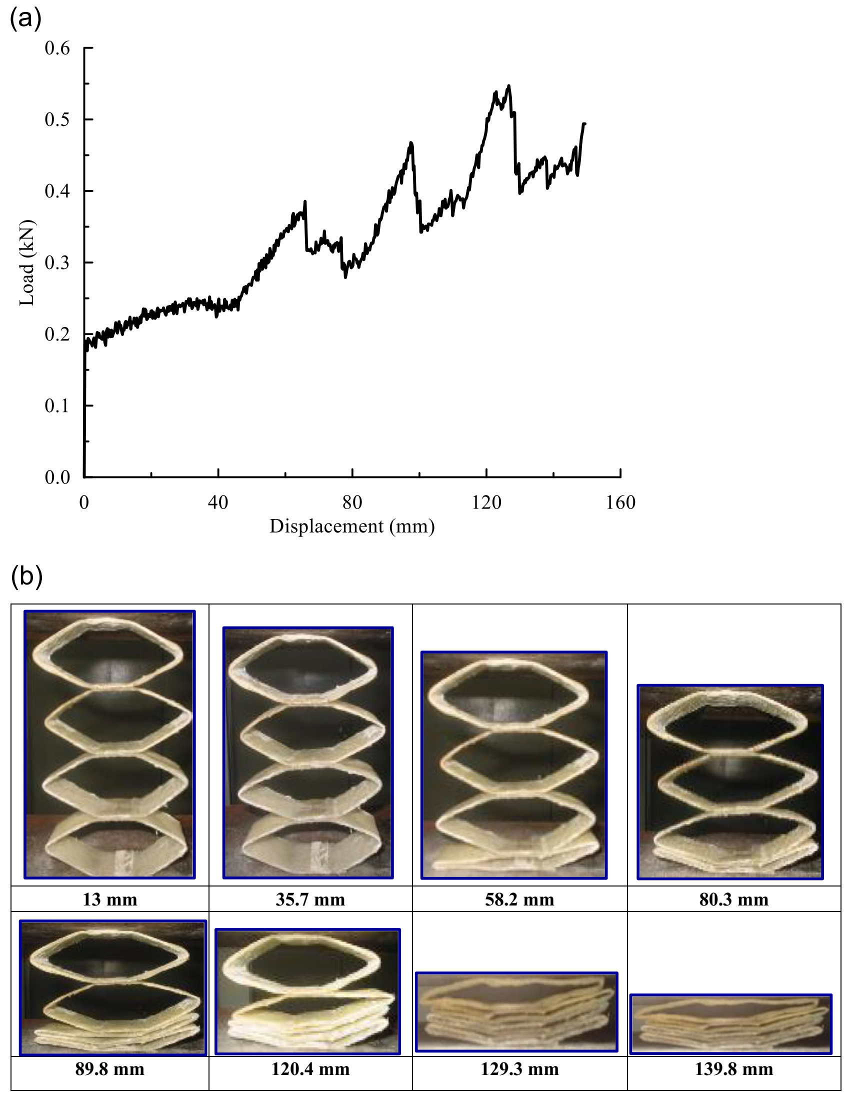

Figure 10. (a) The load–displacement curve for composite hexagonal quadruple ring system with angle 60°. (b) Representative-photographs have been taken during different stages of deformation history of composite hexagonal quadruple ring system with angle 60°, crushing sequence (E_L-M_L-M_U-E_U).

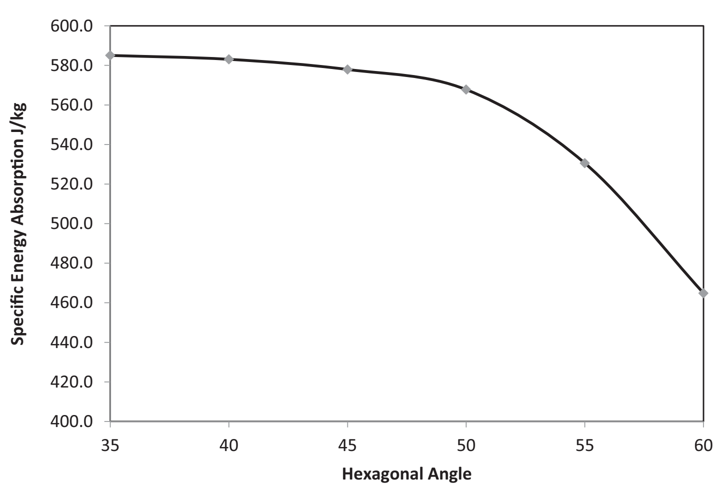

Figure 11. Specific energy absorption capability vs. hexagonal angle.

locations where several fibers debond from the matrix under load. The matrix crack growth process is probably time-dependent, one should relate the crack growth rate to loading history (see Figure 12). It is also well known that in most continuous fiber cross-ply composite laminates, transverse matrix cracking or micro-cracking takes place in the 90° plies at strain levels, which are very small, compared to the ultimate failure strain of the composite laminate; W_{fd} is

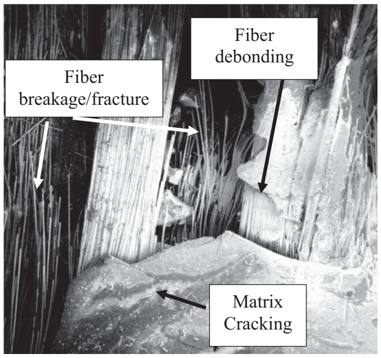

Figure 12. Characteristic fracture morphologies after inplane crushing tests show matrix cracking, fiber debonding and fiber breakage.

the energy required to debond the woven roving fabric fiber from the matrix (see Figure 12); W_{bf} is the energy required to fracture the fibers (see Figure 12).

5. Conclusions

In the current paper, different configurations of one dimensional quadruple hexagonal systems were manufactured and experimentally tested under in-plane quasistatic crushing load. The following conclusions can be drawn:

- The load–displacement response of the 1×4 quadruple hexagonal systems is significantly affected by cell angle, and as the angle increases, the specific energy (E_s) absorbed decreases.
- The cell shape significantly affected the crushing sequence of 1×4 quadruple hexagonal systems. As the hexagonal angle increases, the crushing sequence of the systems changed from the middle to the end cells.
- Despite the change of crushing history sequence, the progressive failure mode was observed for all tested specimens.
- A quadruple hexagonal system with the hexagonal angle of 35° recorded the highest energy absorption capacity.

Disclosure statement

No potenial conflict of interest was reported by the authors.

References

[1] Johnson W, Walton A. Protection of car occupants in frontal impacts with heavy lorries: frontal structures. Int J Impact Eng. 1983;1:111–123.
[2] Mahdi E, Eltai E. Development of cost-effective composite repair system for oil/gas pipelines. Compos Struct. 2018;202:802–806.
[3] Abdewi EF, Sulaiman S, Hamouda AMS, et al. Effect of geometry on the crushing behaviour of laminated corrugated composite tubes. J Mater Process Technol. 2006;172:394–399.
[4] Mahdi E, Sebaey TA. An experimental investigation into crushing behavior of radially stiffened GFRP composite tube. Thin-Walled Struct. 2014;76:8–13.
[5] Alkateb M, Mahdi E, Hamouda AMS, et al. On the energy absorption capability of axially crushed composite elliptical cones. Compos Struct. 2004;66:495–501.
[6] Klaus M, Reimerdes H-G, Gupta NK. Experimental and numerical investigations of residual strength after impact of sandwich panels. Int J Impact Eng. 2012;44:50–58.
[7] Greve L, Pickett AK, Payen F. Experimental testing and phenomenological modeling of the fragmentation process of braided carbon/epoxy composite tubes under axial and oblique impact. Compos Part B. 2008;39:1221–1232.
[8] Bisagni C, Di Pietro G, Fraschini L, et al. Progressive crushing of fiber-reinforced composite structural components of a formula one racing car. Compos Struct. 2005;68:491–503.
[9] Bisagni C. Experimental investigation of the collapse modes and energy absorption characteristics of composite tubes. Int J Crashworthiness. 2009;14:365–378.
[10] Saito H, Chirwa EC, Inai R, et al. Energy absorption of braiding pultrusion process composite rods. Compos Struct. 2002;55:407–417.
[11] Yan L, Chouw N. Crashworthiness characteristics of flax fiber reinforced epoxy tubes for energy absorption application. Mater Design. 2013;51:629–640.
[12] Mahdi E, Hamouda A, Sahari B, et al. Effect of hybridization on crushing behavior of carbon/glass fiber/epoxy circular–cylindrical shells. J Mater Process Technol. 2003;132:49–57.
[13] Abosbaia A, Mahdi E, Hamouda A, et al. Energy absorption capability of laterally loaded segmented composite tubes. Compos Struct. 2005;70:356–373.,
[14] Gupta NK, Abbas H. Lateral collapse of composite cylindrical tubes between flat platens. Int J Impact Eng. 2000;24:329–346.
[15] Hamada H, Coppola J, Hull D, et al. Comparison of energy absorption of carbon/epoxy and carbon/PEEK composite tubes. Composites. 1992;23:245–252.
[16] Mamalis A, Manolakos D, Ioannidis M, et al. Crashworthy characteristics of axially statically compressed thin-walled square CFRP composite tubes: experimental. Compos Struct. 2004;63:347–360.
[17] Meran AP, Toprak T, Muğan A. Numerical and experimental study of crashworthiness parameters of honeycomb structures. Thin Walled Struct. 2014;78:87–94.
[18] Mamalis A, Manolakos D, Ioannidis M, et al. The static and dynamic axial collapse of CFRP square tubes: finite element modeling. Compos Struct. 2006;74:213–225.
[19] Haorongbam H, Deb A, Gupta NK. Behavior of polyurethane foam-filled steel hat under axial loading: testing and Simulation. Procedia Eng. 2017;173:1349–1356.
[20] Elgalai A, Mahdi E, Hamouda A, et al. Crushing response of composite corrugated tubes to quasi-static axial loading. Compos Struct. 2004;66:665–671.
[21] Mahdi E, Hamouda A, Mokhtar A, et al. Many aspects to improve damage tolerance of collapsible composite energy absorber devices. Compos Struct. 2005;67:175–187.
[22] Abosbaia A, Mahdi E, Hamouda A, et al. Quasi-static axial crushing of segmented and non-segmented composite tubes. Compos Struct. 2003;60:327–343.
[23] Mahdi E, Hamouda A. Energy absorption capability of composite hexagonal ring systems. Mater Des. 2012;34:201–210.
[24] Jimenez M, Miravete A, Larrode E, et al. Effect of trigger geometry on energy absorption in composite profiles. Compos Struct. 2000;48:107–111.
[25] Eshkoor R, Ude A, Sulong AB, et al. Energy absorption and load carrying capability of woven natural silk epoxy–triggered composite tubes. Compos Part B Eng. 2015;77:10–18.
[26] Mahdi E, Hamouda A, Sebaey T. The effect of fiber orientation on the energy absorption capability of axially crushed composite tubes. Mater Des. 2014;56:923–928.
[27] Sebaey T, Mahdi E, Shamseldin A, et al. Crushing behavior of hybrid hexagonal/octagonal cellular composite system: all made of carbon fiber reinforced epoxy. Mater Des. 2014;60:556–562.
[28] Alkbir M, Sapuan S, Nuraini A, et al. Effect of geometry on crashworthiness parameters of natural Kenaf fiber reinforced composite hexagonal tubes. Mater Des. 2014;60:85–93.

[29] Alkbir MFA, Salit M. S b, Aziz N. b A, et al. Lateral crushing properties of non-woven kenaf (mat)-reinforced epoxy composite hexagonal tubes. Int J Precis Eng Manuf. 2016;17:965–972.
[30] Chiu LN, Falzon BG, Ruan D, et al. Crush responses of composite cylinder under quasi-static and dynamic loading. Compos Struct. 2015;131:90–98.
[31] Esnaola A, Tena I, Aurrekoetxea J, et al. Effect of fiber volume fraction on energy absorption capabilities of E-glass/polyester automotive crash structures. Compos Part B Eng. 2016;85:1–7.
[32] Sun D, Zhang W, Zhao Y, et al. In-plane crushing, and energy absorption performance of multi-layer regularly arranged circular honeycombs. Compos Struct. 2013;96:726–735.
[33] Hussein RD, Ruan D, Lu G, et al. Axial crushing behavior of honeycomb-filled square carbon fiber reinforced plastic (CFRP) tubes. Compos Struct. 2016;140:166–179.
[34] Wang Y, Feng J, Wu J, et al. Effects of fiber orientation and wall thickness on energy absorption characteristics of carbon-reinforced composite tubes under different loading conditions. Compos Struct. 2016;153:356–368.
[35] Rohatgi PK, Kim JK, Gupta N, et al. Compressive characteristics of A356/fly ash cenosphere composites synthesized by pressure infiltration technique. Compos Part A Appl Sci Manuf. 2006;37:430–437.
[36] Gupta PK, Gupta NK. A study on axial compression of tubular metallic shells having combined tube–cone geometry. Thin Walled Struct. 2013;62:85–95.
[37] Gupta NK, Venkatesh. Experimental and numerical studies of impact axial compression of thin-walled conical shells. Int J Impact Eng. 2007;34:708–720.
[38] Hu D, Zhang C, Ma X, et al. Effect of fiber orientation on energy absorption characteristics of glass cloth/epoxy composite tubes under axial quasi-static and impact crushing condition. Compos Part A Appl Sci Manuf. 2016;90:489–501.